International Conference on Space Optics—ICSO 2012

Ajaccio, Corse

9–12 October 2012

Edited by Bruno Cugny, Errico Armandillo, and Nikos Karafolas

Assembly technique for miniaturized optical devices: towards space qualification

Renaud Matthey

Gaetano Mileti

Laurent Stauffer

Philippe Giaccari

et al.

International Conference on Space Optics — ICSO 2012, edited by Bruno Cugny, Errico Armandillo, Nikos Karafolas
Proc. of SPIE Vol. 10564, 105643D · © 2012 ESA and CNES · CCC code: 0277-786X/17/$18 · doi: 10.1117/12.2309064

Assembly Technique for Miniaturized Optical Devices: Towards Space Qualification

Renaud Matthey, Gaetano Mileti
Laboratoire Temps-Fréquence
Institute of Physics, University of Neuchâtel
CH-2000 Neuchatel, Switzerland
Email: renaud.matthey-de-lendroit@unine.ch

Philippe Giaccari
Micos Engineering GmbH
CH- 8600 Dübendorf, Switzerland

Laurent Stauffer
Hexagon Technology Center GmbH
CH-9435 Heerbrugg, Switzerland

Alexandre Pollini, Laurent Balet
CSEM SA
CH-2000 Neuchatel, Switzerland

Abstract—**We present the first steps executed to space qualify an assembly technique for miniaturized optical components that already demonstrated its maturity for the ground segment. Two different types of demonstrators have been manufactured and submitted to various tests: endurance demonstrators placed in simulated environment reproducing strong space environmental constraints that may potentially destroy the devices under test, and a functional demonstrator put in operational conditions as typically found in a satellite environment. The technology, the realized demonstrators and the results of the tests are reported.**

Assembly; micro-optics; SMD; TRIMO; active alignment; laser frequency stabilization; spacialisation

I. INTRODUCTION

There is an increasing demand for the realization of compact, reliable, cost effective and highly stable optical systems for dedicated space applications in interferometers, spectrometers, laser sources, atomic and optical clocks to name a few. Although important efforts of compactness have already been made in some developments [1], further miniaturization is generally desirable to address the severe requirements in terms of mass and volume for space deployment. Here we report on first efforts realized to test and transfer to space environment a well proven robot-driven assembly technique of micro-optical systems used in prototyping and series production, in the perspective of applying it in spatial instrumentation.

II. ASSEMBLY TECHNOLOGY DESCRIPTION

The TRIMO-SMD technique (Three Dimensional Miniaturized Optical Surface Mounted Device) initiated by Hexagon Technology Center GmbH [2] is a mature packaging technology for systems where small optical components must be actively positioned to achieve highly accurate alignment (see Fig. 1).

In a preliminary step, the optical components are mounted individually (glued, clamped or soldered) at abutment with reduced tolerances in relatively simple metal holders. Then, the optical components in holders are actively aligned using a high-precision manipulator with 6 degrees of freedom. Upon completion of the alignment, all degrees of freedom are frozen at once by soldering the holder on a metal base plate with a solder material (see Fig. 2). In this way, compact and lightweight optical systems of high complexity can be assembled.

The holders are monolithic and can be machined easily according to the size and shape of the optics. The solder consists of off-the-shelf washers resting on the base plate and inserted into the holder foot. The base plate is metallic (Arcap, Invar, steel, ...) and serves as basis to the whole assembly. The TRIMO technology requires specific coatings on both sides of the base plate and on the holders for insuring an adequate wetting of the solder. Typical uncertainties (1σ) on final alignment after soldering assembly are $< 0.5\,\mu m$ in translation and < 0.2 mrad in rotation.

III. DEMONSTRATORS FOR SPACE QUALIFICATION

In terms of technology readiness level (TRL) maturity, the TRIMO-SMD technology with metal holders and base plates was considered to be at TRL3. To push forward the readiness level, two complementary demonstrators have been designed, manufactured and submitted to space qualification tests.

A. Description of demonstrators

The first type of device, named endurance demonstrator (ED), was designed to be subjected to strong space constraints, including large temperature ranges and launch simulating vibrations, potentially destructive for the device, and to measure its survival ability. The production cost was specified low to ensure that several copies could be manufactured in view of the

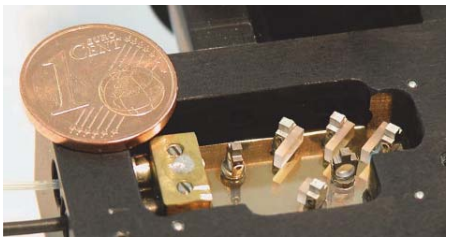

Figure 1. Example of a device with 6 TRIMO elements. The coin (1 cent of €) illustrates the very small size of the TRIMO elements.

This work was supported by the Swiss Secretariat for Education and Research – Swiss Space Office SER-SSO in the frame of the "Mesures d'accompagnement - espace".

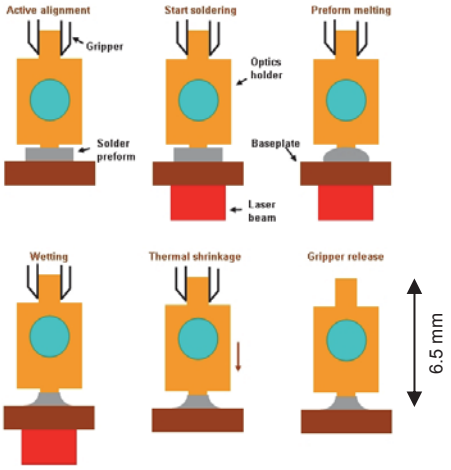

Figure 2. Assembly principle for the TRIMO-SMD technology. See text for a detailed description.

various environmental tests, to ensure representativeness (statistics) and to serve to evaluate the assembly procedure. The device consists of a small mirror fixed to a TRIMO holder which is then placed between two passively aligned reference elements (block mirrors) strongly attached to the base plate. The single actively aligned TRIMO element is based on a proven design already applied previously to develop and test the technology.

The so-called functional demonstrator (FD) device aimed at showing the capability of a relatively complex device based on several TRIMO elements and representing a function to operate in a characteristic space environment, like under vacuum and limited temperature variations, but not under survival conditions. The instrument had to offer the possibility to evaluate rotational misalignments, a very sensitive parameter for some spatial instruments like spectrometers. The FD is built around a saturated absorption scheme, as typically implemented in an atomic Rubidium (Rb) clock to frequency stabilize a semiconductor laser, as illustrated in Fig. 3. The light from a laser is transmitted to the demonstrator through an optical fiber and collimated at the demonstrator entrance by a collimator. The beam is then divided by a beamsplitter. While the unused reflected portion is blocked, the transmitted part (pump beam) passes through a cell containing Rb 87 vapour. A mirror placed after the cell returns the beam back into the cell (probe beam) where it interacts once again with the atoms. The laser light is reflected by the beamsplitter onto a photo-detector. Both the collimator and the cell mirror are attached to TRIMO holders.

For overlapping pump and probe beams, when the laser frequency sweeps an Rb resonance, narrow sub-Doppler resonances features (dips) appear in addition to the Doppler-broadened resonance. The linewidth of the Doppler-broadened resonances and sub-Doppler dips is about 600 MHz and 30 MHz (FWHM), respectively. The dip features hold information on the positioning of the optical elements controlling the laser beam path, as their amplitude and wavelength depend on the superposition geometry of the beams.

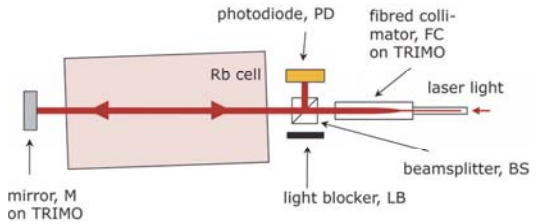

Figure 3. Sketch of the functional demonstrator.

To insure that the results collected with the endurance demonstrator are also valid for the functional demonstrator, the base plate, holders and mirrors have comparable designs for both types of demonstrators.

B. Realisation of demonstrators

Twelve EDs were first assembled. The fabrication process, like the gluing method, could be tested with them and then applied to the manufacturing of four FDs. The EDs also served as perfect test samples to evaluate the variations of the TRIMO holder alignment occurring during the soldering process by measuring the transversal and angular misalignments after soldering. By manufacturing several similar EDs in a row, the soldering process could also be optimized.

1) Endurance demonstrator

Photographs of the ED device are shown in Fig. 4. The pre-assembly operations consisted in fixing the mirror with some adhesive on its TRIMO holder and the two block mirrors on the ED base plate. Jigs were required for passive alignment of the components. After the pre-assembly, the alignment stability of the glued mirrors was tested thoroughly by measuring at different temperatures their angular displacements relatively to a fixed, not glued, large reference mirror using an autocollimation theodolite.

In addition to the manipulator for highly accurate positioning of the TRIMO holder, some measurements tools were added to the standard assembly setup to monitor the position of the holder during the active alignment and to measure the misalignment resulting from the soldering. An autocollimation theodolite served for the angular alignment of the mirror TRIMO holder relatively to the block mirrors, within a resolution better than 5 µrad. A camera equipped with a microscope objective measured the transversal TRIMO holder misalignment due to soldering with 0.1-µm precision.

Defining Y and X as the axes in the base plate plane parallel and perpendicular, respectively, to the beam propagation

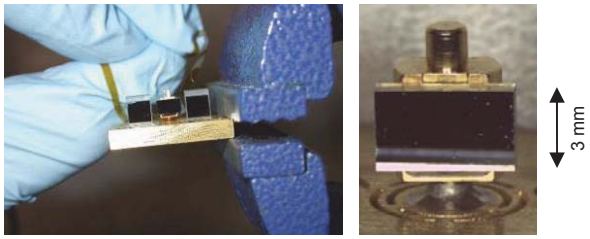

Figure 4. Pictures of a realized endurance demonstrator. (*Left*) Complete device where two reference block mirrors surround the TRIMO holder carrying the test mirror. (*Right*) Enlarged view of the TRIMO holder mirror; the slit structure on the base plate is designed to limit the thermal dissipation. The holder inclusive the optics is a lightweight component (holder: 150 mg; mirror: 40 mg) imposing barely any constrains to the base plate.

direction, Z at 90° to X and Y, H the rotation around Z and V as the rotation around the X axis, the measured uncertainties (1σ) on the alignment after soldering are 0.3 µm along the X axis, 0.4 µm along the Z axis after compensation of the shrinkage, 190 µrad and 60 µrad around the H and V rotation axes, respectively – error on Y could not be measured with this setup. The larger contribution to the holder alignment budget comes from the soldering step.

The thermal stability of the soldered TRIMO holder has been estimated with an autocollimation theodolite. The mirrors glued on their unsoldered TRIMO holders were placed successively in a small insulated enclosure equipped with an optical window. The device under test could be tempered using a Peltier element. The test temperatures were 25°, 60°C, 25°C, 10°C and 25°C. A fixed large mirror served as reference. In average over 10 devices, the thermal stability of the mirror on its unsoldered TRIMO holder remained within an angle of 37 µrad (σ=28µrad). The measurements were repeated once the TRIMO holders were soldered on the base plates. The thermal stability lay then in an angle of 60 µrad (σ=36 µrad), yielding a thermal stability of 23 µrad for the soldered holder itself.

2) Functional demonstrator

The pre-assembly operations for the functional demonstrator consisted in setting up all the components which did not require any active alignment. The components were either mounted by screwing (clamping spring for the Rb cell, photodiode holder, light blocker holder, fiber pull stop) or glued (beamsplitter, light blockers, photodiode, glass block mirrors, cell mirror and collimator on TRIMO holder). An image of the assembled functional demonstrator is shown in Fig. 5.

The fiber pigtail collimator (1.1 mrad full divergence) is an off-the-shelf component based on a gradient index lens. Some adhesives are applied for the fabrication of the pigtail collimators. Depending on the collimator design and on the manufacturing process, the collimator beam pointing stability may vary as a function of temperature. As initial check, the misalignment not directly related to the TRIMO technology was tested. The measured collimator pointing stability between 10°C to 60°C was within an angle of 70 µrad (σ=29 µrad), a value considered as satisfactory for this collimator type.

The collimator TRIMO holder was soldered on the base plate using the robot. The collimator was angularly aligned with an autocollimation theodolite. As reference, a large mirror was clamped on the front face of the base plate. The cell mirror was actively aligned in two successive steps. At first, the holder was adjusted using an autocollimation theodolite considering the reflected signal of the backside cell mirror and the signal reflected from a large mirror clamped against the FD base plate front surface. Then, for the final alignment of the cell mirror, the beam from a laboratory-made laser head was injected into the pigtailed collimator. This laser head, described in more details in [3], contains a single-mode 780-nm DFB laser diode with narrow linewidth (< 4 MHz) and temperature stabilized to a few mK. A temperature-stabilized Rb cell is also implemented in the laser head to serve as frequency reference; frequency stabilities better than 10 kHz over 1 days are reached. By sweeping the laser frequency through the laser current, absorption spectra of the Rb vapor confined in the FD cell were obtained. The alignment merit was monitored by the shape of the fine features in the absorption spectrum (dips).

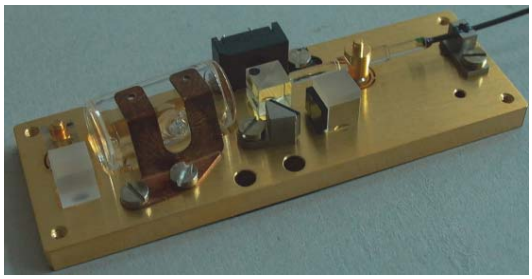

Figure 5. Realized functional demonstrator. The base plate dimensions are 71 mm by 24 mm. See Figure 3 for the description of the components.

IV. TEST DESCRIPTION

The steps followed for a first space validation of the TRIMO-SMD technology are tightly linked to the qualification process that any device built for space applications would have to go through. The EDs served to test the survival ability to the random vibrations endured during a launch for a space mission (breakage and performance reduction), the survival ability to high thermal constraints with specific focus on the soldering of the optical element and to execute a peeling test to investigate the material stability. One of the FDs was used to assess operation in high-vacuum constraint, and sensitivity to temperature. Description and test results for each demonstrator type follow.

A. Endurance demonstrator tests

Among the EDs, one has undergone all tests, some other combinations of tests or only a single test to allow its assessment. One sample has undergone only the transport to the test location and another no test at all to evaluate possible deteriorations due to natural aging of materials.

The launch vibration tests followed strict standard procedures as given by ESA standards (ECSS-E-10-03A). Based on the weight of the device under test and the type of launcher, a vibration power spectral density was determined – flat 0.74 G^2/Hz between 100 Hz and 300 Hz, for an RMS acceleration at the basement of about 24 G (240 m/s²) – and this vibration profile was applied to the device along three coordinated axes during 150 seconds per each axis.

For the aging by temperature cycling tests, the temperature range extended between -30°C and 80 C, limited by the thermal vacuum chamber (TVC) lower reachable temperature, and the maximal temperature where no degradation of the optical component could occur, respectively. This temperature range is already interesting for many earth observation, GNSS and telecommunication satellites. The accelerated aging through thermal cycling tests has been executed in a small TVC at an average pressure of 0.02 mbar. The total number of executed cycles were 33 cycles between -20 and +75°C for a first test leg 1 (test T1) and 111 cycles between -30 and +80°C for a second test leg (test T2). The cycle duration was set to 1h30’ to reach stable high and low temperatures.

Peeling tests have been executed after the environmental testing in order to investigate potential pollution risk from the

TRIMO elements and their soldering due to exposure to harsh environment. The reference standard procedure for the peeling test is reported in ESA standards documentation (ECSS-Q-ST-70-13C). Slight deviations from the standard procedure were needed due to the very small size of the TRIMO samples.

Before the execution of the environmental tests, the relative angular positions between (T-R1) and (T-R2) of the mirrors have been measured, where T, R1 and R2 stand for the TRIMO mirror, reference mirrors 1 and 2, respectively. After the environmental tests, the relative angular position (T'-R1) and (T'-R2) of the mirrors have been re-measured again. The stability of the reference mirrors was measured during the pre-assembly operations; therefore the maximum mirror gluing stability contribution to the TRIMO holder error was known and can be considered in the measurement result interpretation.

B. Functional demonstrator tests

Thermal sensitivity tests were performed to determine the de-alignment susceptibility of the TRIMO holders to temperature based on the fact that the central frequency of a sub-Doppler dip in a Rubidium spectrum depends on the relative angle between the pump and probe beams. Change of this frequency indicates de-alignment occurrence.

The tests were conducted with the FD installed on the temperature controlled base plate of a thermal vacuum chamber (TVC). The laser head deployed during the active alignment of the cell mirror acted as light source; it stayed outside the chamber. The TVC base plate temperature was varied between 10°C and 60°C (a range slightly larger than the one a typical optical instrument operates) in 5°C increments, with sufficient time to allow thermalization of the FD. To study the behavior of the TRIMO technology under vacuum, the thermal sensitivity test was performed for three different pressures: atmospheric pressure, medium vacuum (between $2 \cdot 10^{-2}$ and $9 \cdot 10^{-3}$ mbar) and high vacuum (between $1.7 \cdot 10^{-6}$ and $7.7 \cdot 10^{-6}$ mbar).

In addition to the FD Rb cell absorption signal at each temperature, two other signals were synchronously recorded: a signal linearly proportional to the current ramp and the sub-Doppler absorption spectrum of the Rb cell equipping the laser head, which serves as reference spectrum. Variations of the difference between the frequency of a Doppler-free dip in the reference cell spectrum and the coinciding dip in the FD cell spectrum corresponds to frequency shift linked to angular shift in the FD, as the laser head temperature is well stabilized.

V. RESULTS

A. Endurance demonstrator

The visual inspection of the samples has evidenced no visible changes after the execution of the random vibration tests along the three axes and nothing to report or highlight for all samples. Also, the visual inspection of the samples after the execution of aging by thermal cycling tests T1 and T2 has evidenced no visual changes and nothing to report or highlight. The visual inspection of the samples and the peeling tape after the execution of the peeling tests has evidenced nothing to report or highlight. However, due to the combination of the procedure adopted, the size of the sample and the size of the tape, the tape used had the tendency to roll up at the sampling position. In addition, the area of soldering in contact with the tape was limited. Therefore the contact between the soldering surface and the tape has been performed and adjusted manually, but cannot be fully granted.

The measured displacements after the environmental loads, averaged over the number of samples and over the axes of rotation or axes of translation, are given in Table I.

TABLE I. ED MEASURED DISPLACEMENTS AFTER LOADS

Load	Displacement	Average	σ	# samples
Vibration	Rotation [μrad]	11	53	4
Vibration	Translation[μm]	0	0.53	4
Temperature T1	Rotation [μrad]	14	15	2
Temperature T1	Translation [μm]	0.35	0.25	2
Temperatures T1+T2	Rotation [μrad]	24	64	2
Temperatures T1+T2	Translation [μm]	0.09	1.2	2
Vibration and temperatures T1+T2	Rotation [μrad]	-14	272	1
Vibration and temperatures T1+T2	Translation [μm]	-1	1	1
Transportation and natural aging	Rotation [μrad]	-8	17	2
Transportation and natural aging	Translation [μm]	-0.13	0.18	2

See text for detailed description of the loads.

All ED devices survived the tests; no catastrophic failures and displacements occurred to the EDs. The samples withstood relatively well the vibration load as well as the aging test T1. More critical is the aging test T2. One ED showed a behavior that could not be fully explainable: a very large Z-translation misalignment of -4.3 μm as a consequence of the vibration test. It has been removed from the σ computation. Measurements of the relative position of the reference block mirrors indicated that some of them suffered from misalignments during the environmental loads, what impaired on the TRIMO holder displacement evaluation. For instance, disregarding one ED obviously in this case among the four EDs initially considered in the rotation evaluation for the vibration load, the corresponding 1σ value lowers from 53 μrad to 16.3 μrad.

B. Functional demonstrator

The FD operated without incident during the whole test campaign and data were always collected for all temperatures and pressures. Some spectra recorded at different temperatures are shown in Fig. 6. The resonance signal amplitude depends on the vapor density which on its turn depends on the temperature. Spectra above 50°C are saturated because the vapor density is large enough to completely extinct the laser beam. The signals recorded for the three different pressures look quite much alike (not all shown here).

The data of each spectrum and each cell (FD and laser head) were processed by fitting to precisely retrieve the frequency shifts of the Doppler-free saturated absorption dips in the FD absorption spectrum as a function of temperature and pressure. Each absorption spectrum consists of the sum of a linear slope, a Gaussian-like bell curve, and several Lorentzian-like dips. The linear slope corresponds to the increase in laser

power related to the laser current modulation; the Gaussian curve is actually the Doppler-broadened absorption spectrum of Rb, and the Lorentzian dips are the signature of the Doppler-free saturated absorption.

The frequency shift of the middle dip as a function of the device temperature is presented in Fig. 7. The colors refer to the pressure inside the TVC. From 50 C and above, the dispersion of the results becomes larger because the precision of the fit degrades when the absorption spectra are saturated or near to saturation. At low temperature, the amplitude of the FD signal is smaller, what also increases the uncertainty of the fit and, consequently, the imprecision on the frequency of the dip center. Other sources of uncertainties on the frequency shift include the measurement instrumentation and the laser stability, yet their influence (<± 10 kHz each) is clearly smaller than the fit-induced error (from ±80 kHz up to ~±300 kHz depending on the temperature). From the obtained results, no clear dependency on temperature or pressure can be inferred for the frequency shift of the dip; it is hidden in the error range. Similar results and observations are valid for the two other detected sub-Doppler features.

Measurements realized in the past showed a dependency of about 50 kHz per mrad of change of angle between the pump and probe beams. Assuming this value is also applicable here and considering that the angle between the two beams is twice the mirror rotation angle, the mirror angular alignment is maintained within 2 mrad for temperatures between 20°C and 45°C. More precise values for the temperature (or pressure) dependant angular shift of the TRIMO holder could be achieved by using more sophisticated measurement methods (like heterodyne detection of frequency-locked lasers) or instrumentation (frequency-stabilized optical comb).

Conclusion

In this study, the optical assembly TRIMO technology has been evaluated in view of deployment in the spatial domain. Two types of devices were assembled and set in typical space environments like launch and instrumental operational conditions. No dysfunction of the demonstrators was detected. They ran with high stability despite the sometimes hard operational constrains. All tests (including vibration, extreme temperature range, high vacuum, pilling) were successfully passed and no show-stopper for use of the technology in space could be detected so far. Results indicate that misalignments due to the applied environmental loads are usually smaller than the soldering accuracy which, globally, represents the larger contributor to the alignment uncertainty. Improving further the displacement evaluation approach would lower the error on the alignment retrieval, presently based on glued reference block mirrors.

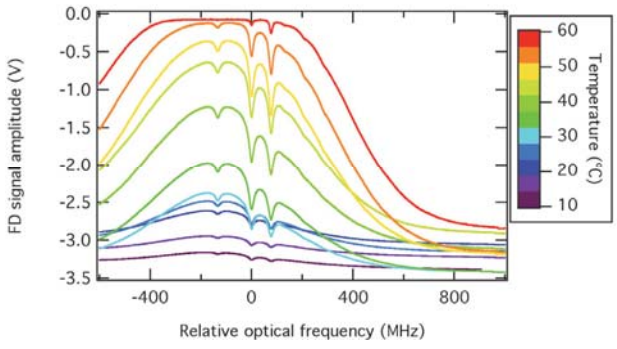

Figure 6. Spectroscopic absorption signals for the functional demontrator recorded for different temperature of the device under high vacuum conditions (<7.7·10^{-6} mbar).

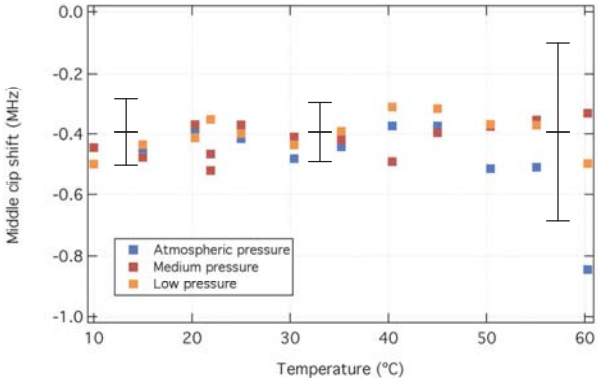

Figure 7. Frequency shift of the middle dip in fonction of the device temperature with respect to the reference frequency from the stable laser head. The errors are ±120 kHz, ±100 kHz and ±300 kHz for temperatures below 20°C, between 20 and 45°C, and from 50°C and above, respectively.

The achieved results augur well for the development of compact, reliable, ruggedized TRIMO-based space-qualified instruments and further spreading of the technology for on-ground applications. Envisaged next steps for the technology concern additional tests for full space qualification (like extended micro-vibration evaluation, radiation or deeper harsh environment testing), and developments of subsystems for space-based instrumentation, e.g., laser transmitter or miniaturized laser frequency stabilization setup [4].

Acknowledgment

The authors thank M. Pellaton, F. Gruet and C. Affolderbach (UniNE-LTF), U. Meier and E. Alberti (Micos), F. Saupe (HTC), J. Bennes and S. Lecomte (CSEM) for their contributions to the work.

References

[1] C. Affolderbach, F. Gruet, R. Matthey, G. Mileti, A compact laser-pumped Rb clock with 5x10^{-13} $\tau^{-1/2}$ frequency stability, Proceedings of the Joint Meeting of the European Frequency and Time Forum and the IEEE Frequency Control Symposium, San Francisco, 2-5 May 2011, pp. 944 – 946 (2011).

[2] L. Stauffer, F. Wälti, U. Vokinger, K. Siercks, High precision surface mount assembly of micro-optical components per laser reflow soldering – positioning accuracy and thermal stability, Proceedings SPIE, vol 5454, pp 85-95 (2004).

[3] C. Affolderbach, G. Mileti, "A comparct laser head with high frequency stability for Rb atomic clocks and optical instrumentation," Review of Scientific Instr., vol. 76, 073108, July 2005.

[4] R. Matthey, S. Schilt, D. Werner, C.Affolderbach, L. Thévenaz, G. Mileti, "Diode laser frequency stabilisation for water-vapour differential absorption sensing", Appl. Phys. B 85 (2-3), 477-485 (2006)